Coupling an Advanced Land Surface–Hydrology Model with the Penn State–NCAR MM5 Modeling System. Part II: Preliminary Model Validation

FEI CHEN AND JIMY DUDHIA

National Center for Atmospheric Research, Boulder, Colorado

(Manuscript received 14 February 1999, in final form 25 July 2000)

ABSTRACT

A number of short-term numerical experiments conducted by the Penn State–NCAR fifth-generation Mesoscale Model (MM5) coupled with an advanced land surface model, alongside the simulations coupled with a simple slab model, are verified with observations. For clear sky day cases, the MM5 model gives reasonable estimates of radiation forcing at the surface with solar radiation being slightly overestimated probably due to the lack of aerosol treatment in the current MM5 radiation scheme. The improvements in the calculation of surface latent and sensible heat fluxes with the new land surface model (LSM) are very apparent, and more importantly, the new LSM captures the correct Bowen ratio. Evaporation obtained from the simple slab model is significantly lower than observations. Having time-varying soil moisture is important for capturing even short-term evolution of evaporation. Due to the more reasonable diurnal cycle of surface heat fluxes in the MM5–LSM, its near-surface temperature and humidity are closer to the FIFE observations. In particular, the MM5–slab model has a systematic warm bias in 2-m temperature. Both the slab model and the new LSM were coupled with the nonlocal Medium-Range Forecast model PBL parameterization scheme and they reproduced the depth of the morning surface inversion in the stable boundary layer well. The observed mixed layer in the late morning deepens faster than both models, despite the fact that both models have high bias in surface sensible heat fluxes. Presumably, such a rapid development of convective mixed layer is due to some effects induced by small-scale heterogeneity or large-scale advection that the MM5 failed to capture. Both surface models reasonably reproduce the daytime convective PBL growth and, in general, the temperature difference between the two models and observations is less than 2°. The simulations of two rainfall events are not conclusive. Both models produce a good forecast of rainfall for 24 June 1997 and have similar problems for the event of 4 July 1997, although the simulations with the new LSM have slightly improved results in some 3-h rainfall accumulations. It seems that the new LSM does not have unexpected influences in situations for which the land surface processes are secondary, but that it may have subtle, though complex, effects on the model behavior because of heterogeneity introduced by soil moisture, vegetation effects, and soil type, which are all lacking in the slab model.

1. Introduction

This is the second paper in the series presenting our effort in coupling an advanced land surface model (LSM) with the Pennsylvania State University–National Center for Atmospheric Research (Penn State–NCAR) fifth-generation Mesoscale Model (MM5) system and in validating this coupled system. In the first paper (Chen and Dudhia 2001, hereafter Part I), we have addressed several issues related to the MM5–LSM coupling strategy, which involves the implementation of an LSM, the introduction of 1-km resolution annually fixed vegetation and soil maps, seasonally varying green vegetation fraction, the specification of various parameters related to the soil and vegetation types, and soil moisture initialization procedures. In this paper, we focus on the evaluation of this coupled system by comparing model simulations with data obtained from field observations.

Validating the performance of the land surface physics component as embedded in a three-dimensional modeling system is not a straightforward task. Note that a land surface model only provides surface sensible and latent heat fluxes as lower boundary conditions to the coupled atmospheric model. These heat and moisture fluxes are then transported throughout the boundary layer, and interact with other model physics involving cloud, radiation, and precipitation processes. In such a complex and highly nonlinear modeling system, errors in one of the above physical parameterization, whether vegetation parameterizations, surface layer physics, or planetary boundary layer (PBL), can all interact to result in an erroneous diurnal cycle of the mixed layer, and it is difficult to separate the surface processes from other physical processes. However, if we concentrate on the

Corresponding author address: Fei Chen, National Center for Atmospheric Research, P.O. Box 3000, Boulder, CO 80307.
E-mail: feichen@ncar.ucar.edu

parameters close to the ground surface and within the boundary layer where the underlying surface processes exert important influences, the effects of land surface model can be assessed.

Given the fact that this is the first advanced land surface model ever implemented in the official NCAR-supported release of the widely used Penn State–NCAR MM5 modeling system, the intent of this paper is to provide some documentation of the performance of the current simple slab model and the advanced LSM. In particular, we will evaluate the MM5's ability to reproduce the observed diurnal cycle of the mixed layer with a fully coupled surface and boundary layer for several selected cases. Hence, in this paper, we will first examine the behavior of the land surface model under clear sky situations so that the surface forcing conditions, particularly the surface radiation components, are not biased by the model prediction of clouds. It is still difficult for MM5, or any other mesoscale model for that matter, to capture the evolution of clouds at small scales. Also, it is necessary to validate the area-averaged surface heat fluxes that the mesoscale models are supposed to produce. The data collected during the First International Satellite Land Surface Climatology Project (ISLSCP) Field Experiments (FIFE) (Sellers et al. 1992), and especially the surface heat fluxes, averaged over the 15×15 km^2 FIFE observation domain, provide a valuable opportunity to perform this type of verification. This high quality dataset has been used to validate the simulations of large-scale and mesoscale models (e.g., Betts et al. 1993, 1997, etc.). The evolution of the PBL is also investigated to demonstrate the influence of changes in the surface energy partition on the development of the convective PBL. Finally, two precipitation cases are examined.

2. Validation data

a. FIFE observations

Extensive surface data were collected over the Konza prairie in Kansas during the FIFE experiment (Sellers et al. 1992). The 1987 FIFE data used in this study are area-averaged observations, which are based on the 30-min spatial mean time series derived by Betts and Ball (1998) by averaging data collected over different stations in the FIFE area of 15 km $\times$ 15 km. The Portable Automated Mesonet (PAM) station time series data (30-min averages at about 10 stations) consisted of atmospheric data such as wind, air temperature and humidity, precipitation, incoming and reflected solar radiation, net radiation and incoming longwave radiation, a radiometric measure of the ground surface temperature, and soil temperature at 10 and 50 cm below the surface.

This dataset also includes the spatial-mean surface sensible heat, latent heat, and ground heat fluxes averaged over 17 selected surface flux stations, which made measurements using both eddy correlation and Bowen ratio methods (Betts et al. 1993). These surface flux stations also measured the aforementioned four radiation components and net radiation. According to Betts et al. (1993), the radiation averages obtained from the flux stations, which have lower incoming solar radiation and a higher albedo, are internally more self-consistent than the radiation data obtained from the PAM stations. The upper-air temperature and humidity data were from the visually tracked radiosondes (Sugita and Brutsaert 1990), which were launched roughly every 90 min. As in Betts et al. (1997), we used the sonde data interpolated to standard 5-mb levels available from Strebel et al. (1994).

b. NCEP 4-km national precipitation analysis

A prototype, real-time, hourly, multisensor National Precipitation Analysis (aka National Stage II analyses) has been developed at the National Centers for Environmental Prediction (NCEP) in cooperation with the Office of Hydrology (OH). This analysis merges two data sources that are currently being collected in real time by the OH and NCEP (Baldwin and Mitchell 1997). Approximately 3000 automated, hourly raingauge observations are available over the contiguous 48 states from the Automated Surface Observing System and via the Geostationary Operational Environmental Satellite Data Collection Platform. In addition, hourly digital precipitation (HDP) radar estimates are obtained as compressed digital files via the Automation of Field Operations and Services network. The radar observation network consists of over 90 Weather Surveillance Radar 1988-Doppler (WSR-88Ds), which report hourly precipitation in real time. The HDP estimates are created by the WSR-88D Radar Product Generator on a 131 $\times$ 131 4-km grid centered over each radar site. The data analysis routines, including a bias adjustment of the radar estimates using the gauge data, have been adapted by NCEP to a national 4-km grid from algorithms developed by OH (Stage II) and executed regionally at National Weather Service at River Forecast Centers.[1]

3. Model configuration

Two sets of numerical experiments were conducted for several cases for 1987 and 1997, respectively. Four control simulations were designed for the 1987 case in order to verify the model against the FIFE observations. The nonhydrostatic MM5 model was run for 48 h for the following four selected cases: 1) 0000 UTC 4 June–0000 UTC 6 June (a clear sky day), 2) 0000 UTC 24 June–0000 UTC 26 June (a convective rain case), 3) 0000 UTC 9 August–0000 UTC 11 August (a cloudy

[1] The 4-km National Precipitation Analysis used in our study is obtained from NCEP archive, which is available online at http://www.emc.ncep.noaa.gov:/mmb/gcp/htmls/hdpprec.html.

day), and 4) 0000 UTC 12 August–0000 UTC 14 August (a large-scale rainfall case). Two 48-h MM5 simulations were conducted for the 1997 case study: 1) 0000 UTC 24 June–0000 UTC 26 June, and 2) 0000 UTC 4 July–0000 UTC 6 July, both having large-scale frontal precipitation. In addition, a number of sensitivity tests were conducted to test the sensitivity of the coupled MM5 model to the specification of soil moisture. These sensitivity studies will be discussed later. Originally, the 1997 experiment set was designed to validate the model results against the Atmospheric Radiation Measurement (ARM) program's Southern Great Plains 1997 data (SGP-97). But the surface heat flux data that we obtained from SGP-97 Web site contained significant errors, and these raw data should be subject to some quality control procedures before being used for this type of validation. Hence, we primarily use the 1997 cases to test the possible MM5 model sensitivity on the larger scale to the treatment of land surface processes, validating primarily against rainfall analysis.

These simulations used 23 vertical levels (with the model top at 100 mb) and three horizontal domains nested with two-way interaction with grid sizes of 90, 30, and 10 km. The outermost domain covers the 48 contiguous states, while the inner 10-km domain is centered on, respectively, the FIFE site in Kansas (for 1987 simulations) and the ARM Southern Great Plains site in Oklahoma (for 1997 simulations). The inner domains cover regions of 510 km by 480 km, while the 30-km domain covers a square of about 1700 km covering most of the region between the Rockies and the Mississippi River.

The 1987 numerical experiments were initialized with data from the NCEP–NCAR reanalyses and provided with 12-hourly boundary conditions on the coarsest domain from those analyses. The coarse-mesh analysis was enhanced by standard upper-air and surface observations available in the NCAR data archives. The analyzed grids were then interpolated to the finer meshes.

For the 1997 experiments, the data come from the relatively high-resolution Eta Model Data Assimilation System analyses (these data are only available for the period 1996–present in the NCAR data archives), so there was no need for a further observational analysis, and the outer two domains were interpolated from the NCEP EDAS output with 40-km horizontal grid spacing, then the 10-km domain was interpolated from the 30-km domain. We used two techniques of implementing this dataset. The first was to use the Eta forecasts to provide boundary conditions 6 hourly, and the second was to use only the 12-hourly analyses. The difference in the interior of the domains was small, and we will report on only the latter method's results here.

The model physics in all runs reported here was cloud-interactive radiation and simple ice microphysics (Dudhia 1989), the Grell convective scheme (Grell et al. 1994), and the Medium-Range Forecast (MRF) model planetary boundary layer scheme (Hong and Pan 1996). Note that other physics options (e.g., Kain–Fritsch and Betts–Miller schemes for cumulus parameterization, Blackadar nonlocal scheme, and Burk–Thompson TKE scheme for PBL, etc.) are available in the MM5, and the MM5 simulation results will certainly depend on, to some extent, the physics option used. We selected the above options because they are used in some operational MM5 applications (e.g., see Davis et al. 1999). The advanced LSM used in the MM5 system is based on the diurnally dependent Penman potential evaporation approach of Mahrt and Ek (1984), the multilayer soil model of Mahrt and Pan (1984), and the primitive canopy model of Pan and Mahrt (1987). It has been extended by Chen et al. (1996) to include the modestly complex canopy-resistance approach of Jacquemin and Noilhan (1990) and the surface runoff scheme of Schaake et al. (1996). It has one canopy layer, and the following prognostic variables: volumetric soil moisture and temperature in four soil layers, water stored on the canopy, and snow stored on the ground. Four soil layers are employed, where the thicknesses of the layers are 0.1, 0.3, 0.6, and 1.0 m, from the top layer to the bottom layer, respectively. The root zone is in the upper 1 m of soil, and the lower 1 m of soil acts like a reservoir with gravity drainage at the bottom (more details on the new LSM are in Part I of this paper). An alternative that is simpler than the LSM for representing the surface energy and moisture budgets, and their response to landscape variability, is also tested. This simpler approach employs the ''slab model'' developed by Blackadar (1976, 1979) and further tested by Zhang and Anthes (1982). Ground temperature is calculated from a more recent five-layer soil thermal diffusion option (with layer's thicknesses of 1, 2, 4, 8, and 16 cm), and there is no explicit representation of vegetation effects. The soil moisture remains constant during a simulation, and is defined in terms of a moisture availability that depends on land use type.

The land use map was from the U.S. Geological Survey 1-km Advanced Very High Resolution Radiometer derived dataset, using a single dominant type in each model grid box. The 16-class Simple Biosphere Model categories were used and mapped to the original MM5's 13 categories for the purposes of assigning roughness length and albedo for both surface models, and emissivity, moisture availability, and thermal inertia for the slab model. In the land surface model the emissivity is taken to be unity for the skin temperature, and soil thermal properties depend on a separate soil-type dataset State Soil Geographic Database (STATSGO) for some comparison tests. As mentioned in Part I, both the NCEP-NCAR Reanalysis Project (NNRP) and EDAS analyses contain the necessary soil moisture and temperature information from a land surface model that is compatible with the one used here. However the NNRP soil moistures were corrected for known biases as described before.

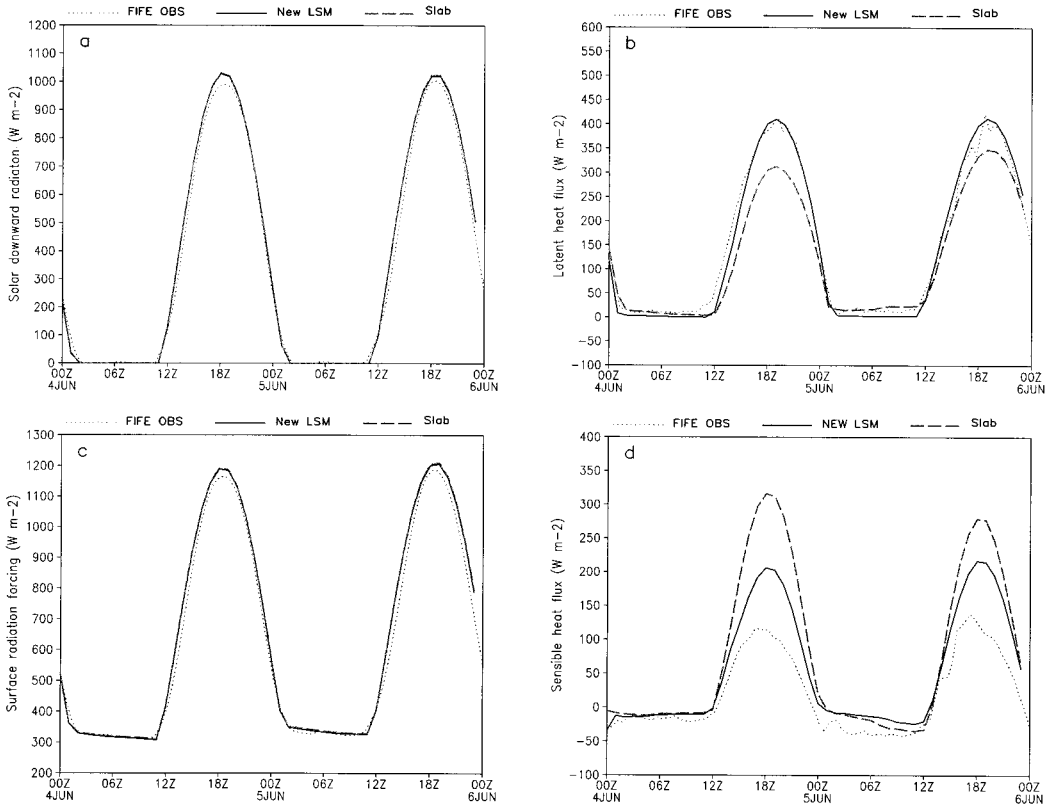

FIG. 1. Comparison between simulations by two coupled models and FIFE observations: (a) downward solar radiation; (b) latent heat flux; (c) surface radiation forcing, which is the sum of net downward solar radiation and downward longwave radiation; and (d) sensible heat flux. FIFE, FIFE observations; New LSM, MM5 simulation with the new LSM; and Slab, MM5 simulation with the simple slab model.

4. Comparison results and discussions

a. Validation of model surface heat fluxes

We compare 48-h forecasts from the two different configurations of the MM5 model for the grid point (the grid spacing is 10 km in domain 3) near the FIFE site with the observed near-surface meteorological data and surface heat fluxes. This tests the ability of the fully coupled model to reproduce the observed land surface diurnal cycle. Figures 1 and 2 show the diurnal cycle of a 2-day period simulated by two versions of the MM5 model for the 4 June 1987 (a clear sky day) case. The initial soil moisture in the MM5–LSM, based on NCEP–NCAR reanalysis (Kalnay et al. 1996), and the surface moisture availability in the slab model are both wet, although the two preceding days had been rain free in the reanalysis. These two days are similar undisturbed days with little cloud cover.

Both the model results and observations are plotted at 30-min time intervals. The downward solar radiation simulated by the two models is similar, and agrees with observations well, except the slight overestimation (about 20–40 W m^{-2}) near the local noontime. Such an overestimation of downward solar radiation under clear sky conditions is fairly common in mesoscale models and has been reported by others (e.g., Betts et al. 1997). One probable reason for this is the lack of aerosol treatment in the current MM5 radiation scheme. This overestimated downward solar radiation is also reflected in the surface radiation forcing. Thus, both models have a slightly higher surface radiation forcing than observations (see Fig. 1c). Also, the MM5 model captures fairly well the downward longwave radiation at the surface (not shown here). Noticeably, the observed surface radiation forcing at night (Fig. 1c) is reasonably reproduced by both models, indicating a good estimation of nighttime downward longwave radiation at the surface.

Compared to the FIFE observations, the improvement in the calculation of surface heat fluxes with the new LSM is very apparent. The observed maximum latent heat flux is about 400 W m^{-2} on both days. The new LSM captures the correct Bowen ratio (the ratio of sensible heat flux to latent heat flux), which is usually small during this vegetation growing season when a large portion of incoming energy is used for vegetation evapotranspiration. Latent heat fluxes calculated by the simple slab model are significantly lower than observations with a maximum difference of about 100 W m^{-2} around the local noontime. In this particular case, the initial soil moisture in the slab model may be responsible for such

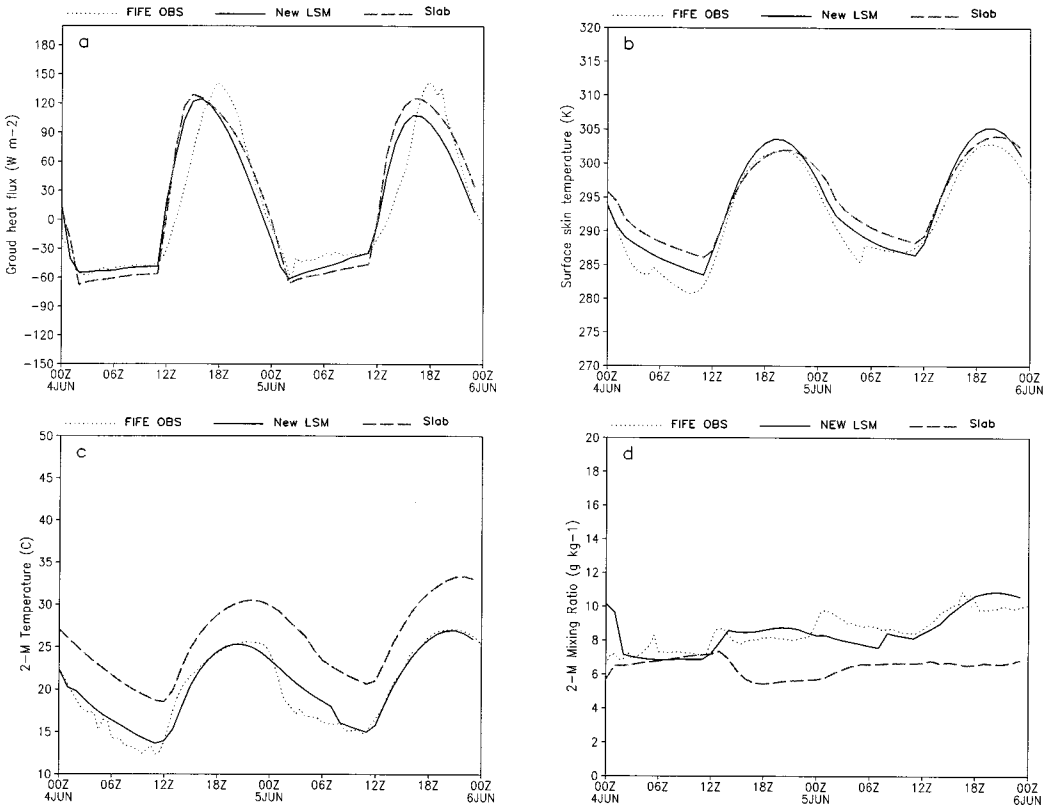

FIG. 2. Same as Fig. 1 but for the following variables: (a) ground heat flux, (b) surface skin temperature, (c) 2-m air temperature, and (d) 2-m air mixing ratio.

underestimation. In fact, modeling latent heat flux is more difficult because of complex interactions among plant physiology and the evapotranspiration process, and hence utilizing only the surface moisture to determine the evaporation rate in the slab model cannot correctly represent the influence of environmental conditions and that of deep root zone soil moisture on the canopy resistance.

Figure 1d shows the corresponding surface sensible heat flux comparison. The observed sensible heat flux is relatively low in early summer with a peak of 100–130 W m^{-2} due to high evaporation in this region. Although the simulation of sensible heat fluxes with the new LSM is closer to the FIFE observations than that with the slab model, both models overestimated them. It also seems that the soil heat fluxes in the two models are similar and reached their maximum earlier than observations (Fig. 2a). This type of phase lag (i.e., with an early peak of ground heat flux) seems a common problem in land surface modeling. For instance, T. H. Chen et al. (1997) compared offline simulations by 23 land surface models to Cabauw observations and noticed that most models produced the early peak in ground heat fluxes, which may be due to a delayed transfer of soil temperature information into the atmospheric boundary layer calculations. One interesting feature in this comparison is that the latent heat flux in MM5–LSM stays nearly the same with a slight reduction on the second day because of the depletion of soil moisture in the vegetation root zone, which agrees with observations. But the opposite is apparent in the MM5–slab model results because of the time-constant soil moisture, other conditions being equal.

One problem, which further complicates the validation of model results against observed surface heat fluxes, is that the surface energy balance is usually not preserved in field data but is always preserved by the model. The surface net radiation (Rnet) is partitioned into latent heat (LE), sensible heat (H), and ground heat (G) fluxes, and, hence, heat flux residuals R (R = Rnet $-$ LE $-$ H $-$ G) should theoretically equal zero. Independent measurements of individual surface flux components usually do not assure the surface energy balance. As shown in Fig. 3, residuals of the above surface energy balance in this case can be 15 W m^{-2}. It is not easy to distinguish model biases from uncertainties in the data themselves and, therefore, some caution must be taken when quantitatively verifying the individual components of surface energy balance. Despite this uncertainty in data, this type of verification can still provide valuable insights into the model parameterization of surface and PBL processes.

The diurnal amplitude of surface skin temperature in the new LSM (Fig. 2b), which is calculated from the

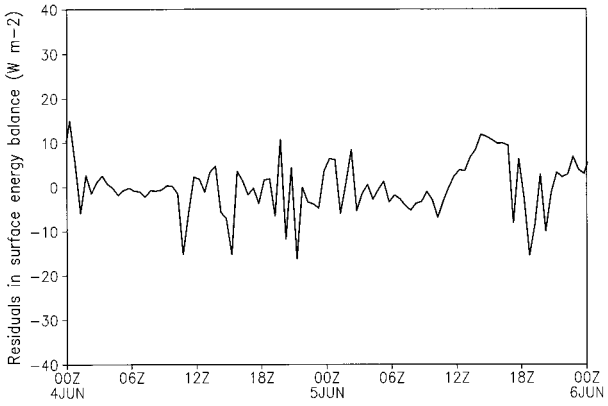

FIG. 3. Residuals in observed surface energy heat fluxes.

surface energy balance, seems to agree with the observations better than that in the slab model, and the latter tends to have a smaller diurnal cycle. This may be due to the fact that the ground temperature in the slab layer, which was taken as surface temperature for the sake of comparison, has thermal inertia for a finite depth (1 cm) of soil. During daytime, the new LSM produces slightly higher (2°–3° most of the time) surface skin temperature than observations. Nevertheless, the surface skin temperature and slab-layer temperature are important parameters in computing the surface energy balance, because they are used to calculate the upward longwave radiation at the surface. Moreover, the surface skin temperature can be easily derived from satellite observations, which provides another tool to verify the coupled model at continental scales. Meanwhile, the slab ground temperature serves a dual role as a radiative temperature and in calculating surface sensible heat fluxes, as well as representing a soil 1-cm-layer temperature.

Examining near-surface variables in the coupled model gives insight into whether the land surface and boundary layer parameterizations interact properly. With a more reasonable diurnal cycle of surface heat fluxes in the new LSM, it is not surprising to see that its 2-m air temperature and humidity are closer to observations than those produced by the slab model (Fig. 2c). In particular, while the slab model has a reasonable amplitude of the diurnal cycle of the near-surface temperature, its 2-m air temperature appears to have a systematic warm bias. Despite a high bias in surface skin temperature at local noon, the observed rise of 2-m temperature from morning to noontime in the new LSM is correctly reproduced. However, the fall of 2-m temperature in the late afternoon and nighttime is slightly slower in the new LSM than that in observations, and hence the new LSM is about 1°C warmer than the data. As can be seen in Fig. 2d, the 2-m mixing ratio has a much smaller diurnal variation than the air temperature. Still,

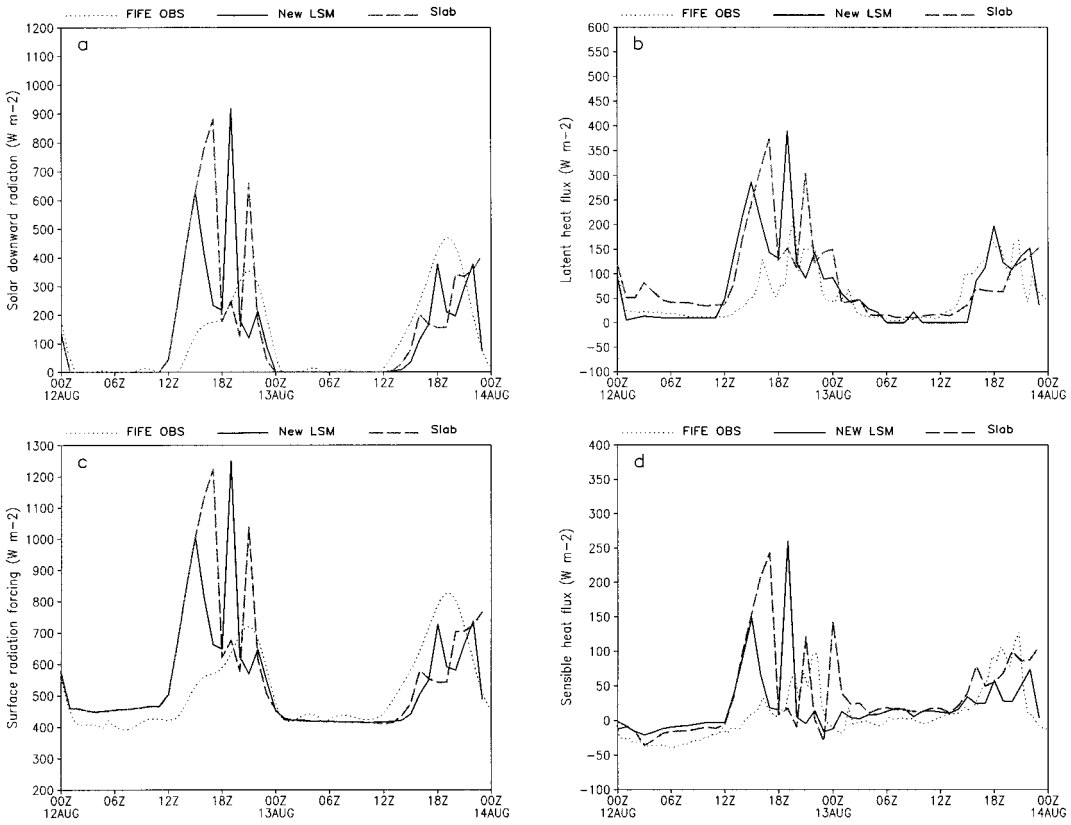

FIG. 4. Same as Fig. 1, but for the 12 Aug 1987 case.

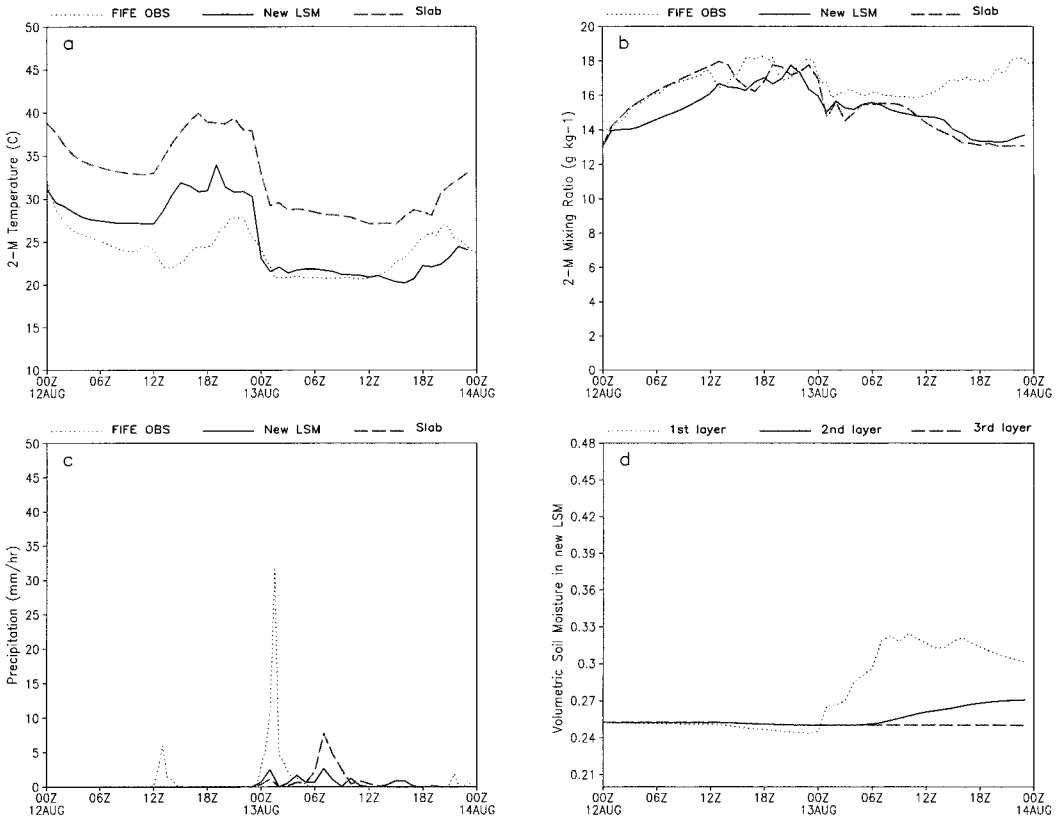

FIG. 5. Same as Fig. 4 but for the following variables: (a) 2-m air temperature, (b) 2-m air mixing ratio, (c) precipitation, and (d) soil moisture change in the three root zone layers of the new LSM.

the data show an increase of surface humidity right after sunrise (probably due to the rapid evaporation of morning dew formed at the surface) and in the afternoon (due to the vegetation evapotranspiration). The new LSM, having the dew process, and more accurate evaporation representation, correctly captures the surface humidity increase during daytime and decrease at nighttime.

The next case shows simulations by the above two models for a day with precipitation over the FIFE area (12–14 August 1987). Figures 4 and 5 compare different components of surface energy balance and near-surface sensible variables between the two model simulations and FIFE observations. This comparison reminds us of the difficulty of modeling local clouds and precipitation in mesoscale models. For instance, model clouds appear too late and too little in the first 18-h forecast, and both models have too much downward solar radiation and net surface radiation forcing (Figs. 4a,c). This may be due to the spinup process, as the cloud is initialized from zero in model simulations. In fact, probably for the same reason, both models do not capture the light rainfall in the first day of simulation (Fig. 5c). This leads to unduly large surface sensible and latent heat fluxes on the first day.

On the second day (13 Aug) of simulation, in contrast to the first day, both models produced too much cloud and resulted in a too little surface radiation forcing at local noontime, which is about 200 W m^{-2} lower than observations. Consequently, surface heat fluxes in both models are underestimated by the same amount. While the forecast of 2-m temperature and humidity was improved in the new LSM (see Fig. 5a), it has a low bias in both temperature and humidity during daytime, due to underestimated surface latent and sensible heat fluxes. Similar but slightly different features are seen in the cases of 24 June and 9 August. For instance, in the case of 9 August, both MM5 simulations produce too much cloud during the first 24 h, and have a high bias (about 80 W m^{-2}) in nighttime downward longwave radiation and low bias in daytime downward solar radiation (not shown here). Hence, both simulations have high bias in nighttime 2-m temperature (about 10 and 5 K warmer than the data for the MM5–slab and MM5–LSM models, respectively).

Figure 5d shows a typical response of root zone soil moisture in the new LSM to evaporation and rainfall. Note that in the slab model the surface moisture availability is defined as function of land use type and hence a spatially varying parameter, but it remains constant during the MM5 simulation period. On the first day, the soil moisture decreases as a result of uptaking water in the root zone by the vegetation evapotranspiration pro-

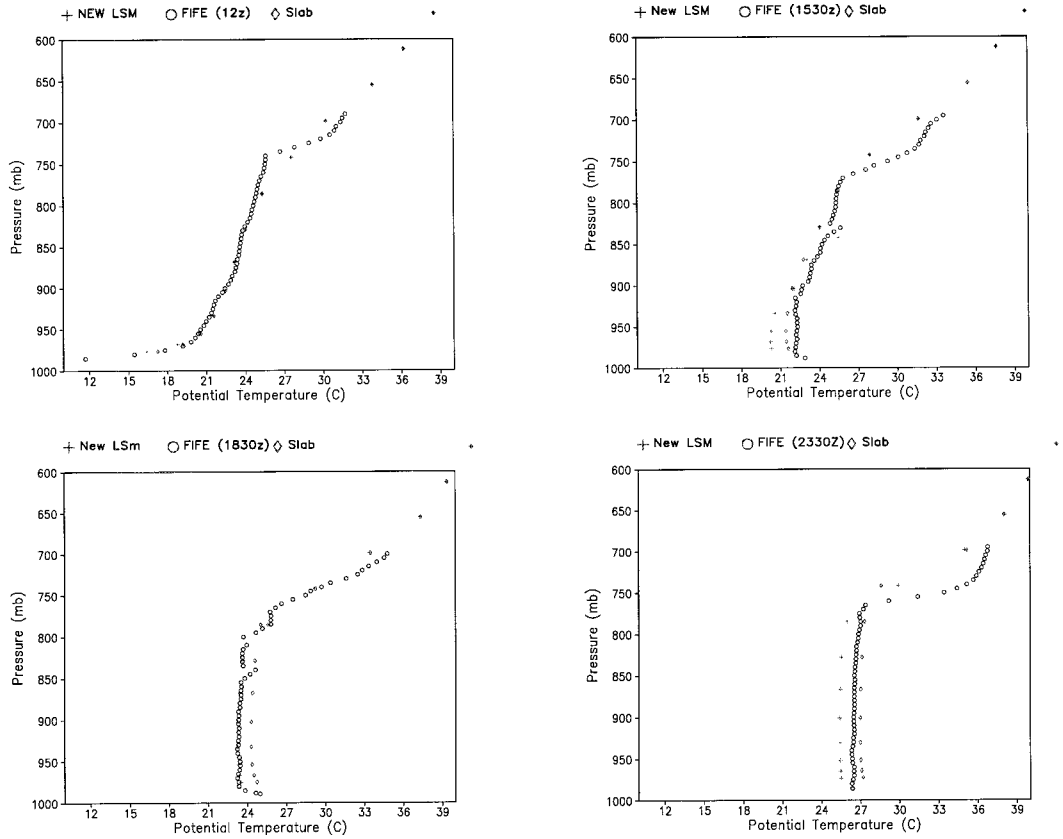

FIG. 6. The vertical profile of PBL potential temperature for 4 Jun 1987: (a) 1200, (b) 1530, (c) 1830, and (d) 2330 UTC.

cess. On the second day, the surface soil moisture, for the depth of 0–10 cm below the ground surface, quickly responds to the rainfall event and is augmented to be close to its field capacity at 0600 UTC 13 August. Once the surface layer is moistened, the hydraulic diffusivity increases and, hence, facilitates the vertical transport of water within the soil (i.e., the drainage process), which increases the soil moisture in the second layer. Usually, for land surface models to capture the daily, weekly, and seasonal evolution of soil moisture, which is critical in long-term soil moisture data assimilation, a multilayer soil model (with at least four levels with appropriate soil level resolution) is required in modern-era coupled models (F. Chen et al. 1997; Viterbo and Beljaars 1995). This level of sophistication is also crucial if MM5 is to be coupled to a hydrology river-routing model in the future.

b. Evolution of temperature and humidity in the boundary layer

We have seen, so far, that the surface heat fluxes and near-surface temperature and humidity simulated by the new LSM are, in general, closer to observations than those produced by the simple slab model. In this section, we investigate the extent to which these changes in surface heat fluxes can modify the diurnal variation of temperature and humidity in the PBL. Discussion is focused on the clear sky day case (i.e., 4 Jun 1987) to avoid the complication caused by differences in clouds simulated by two models. In the following model simulations, both the new LSM and slab models are coupled with the nonlocal PBL parameterization scheme, which was developed by Troen and Mahrt (1986) and has been extensively tested in the NCEP operational Medium-range Forecast model (Hong and Pan 1996).

Figure 6 shows the comparison of the diurnal cycle of the vertical profile of potential temperature between two land surface model simulations and the FIFE radiosondes launched at closely corresponding times on 4 June. The vertical resolution of the sonde data is much finer than that of the MM5 model. At local morning (1200 UTC), both models have the same vertical structure and they agree well with the observations. Note that the model started at 0000 UTC 4 June 1987, so the large-scale initialization conditions, largely based on the NCEP–NCAR reanalysis, in the lower atmosphere are well depicted and MM5 does a reasonable job in simulating the strength and depth of the surface inversion in the stable PBL at 1200 UTC. Although the sensible heat flux is small in FIFE observations (see Fig. 1d), the observed mixing layer deepens faster than both mod-

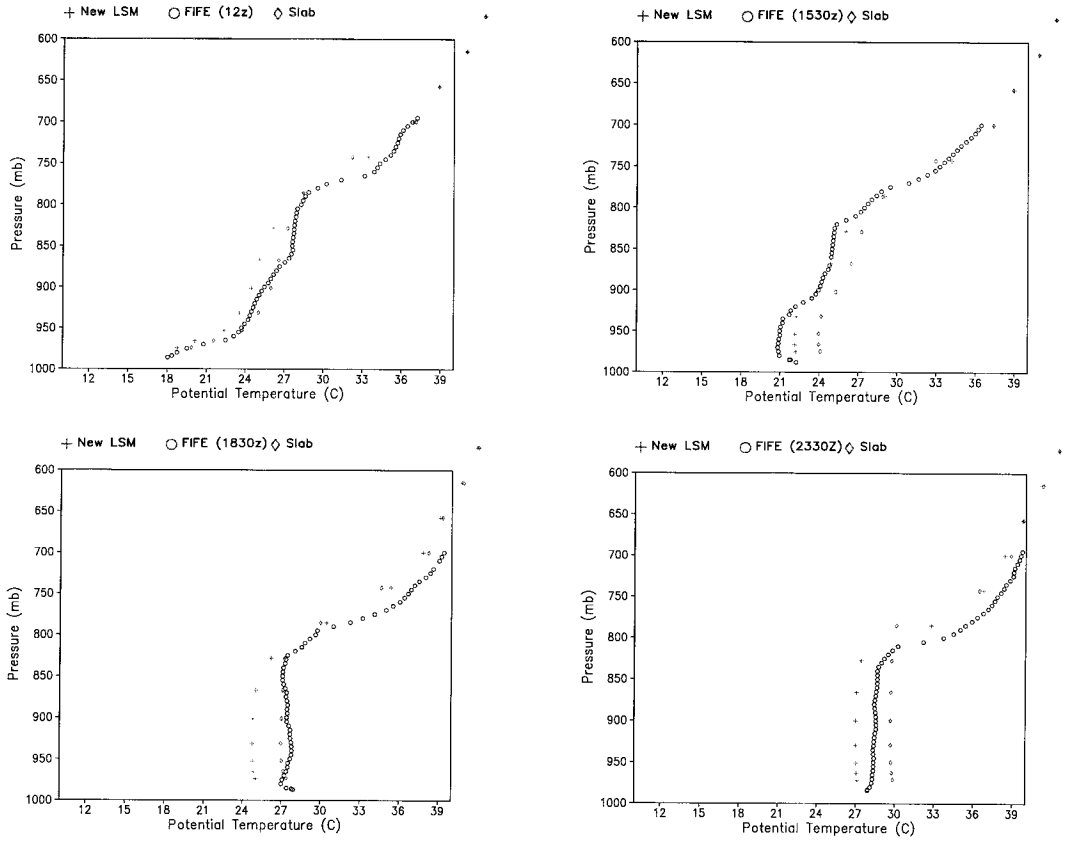

FIG. 7. Same as Fig. 6 but for 5 Jun 1987: (a) 1200, (b) 1530, (c) 1830, and (d) 2330 UTC.

els in the morning, as evidenced in the temperature profile at 1530 UTC. But the model mixing layer in the slab model simulation is warmer than the data at local noontime (1830 UTC), because of too much model sensible heat flux. In fact, the slab model simulation has a warmer boundary layer throughout the day. In the morning (e.g., at 1530 UTC), the influence of surface heat fluxes only reaches the level of 900 mb because of the relatively weak turbulence in the boundary layer, but it rapidly deepens to the 750-mb level in the late afternoon.

At local noontime (1830 UTC), both models fairly well reproduce the vertical structure within the convective mixing layer, but the new LSM simulation agrees better with the FIFE observations. In the afternoon, the mixing layer deepens further into a preexisting deep mixing layer (i.e., the residual mixing layer from the preceding night). The depth of the PBL at 2330 UTC is higher than that at 1830 UTC, and the PBL in the slab (LSM) model simulation is warmer (cooler) than the FIFE observation, but the difference in temperatures among them is usually smaller than 1°C. In general both simulations with different land surface models reasonably capture the daytime development of the PBL, from the morning transition period before 1530 UTC to the fully developed mixed layer at 2330 UTC. For most of the time, the difference between simulations and observations is less than 2°C, indicating a good performance of the MRF PBL scheme.

After a 24-h simulation, both simulations have, again, a good representation of morning surface inversion at 1200 UTC (Fig. 7), but there are slight differences in the residual layer. In contrast to the preceding day (i.e., the first day of the MM5 forecast), the PBL at 1530 UTC in both simulations warms faster than the observed one. The slab model simulation has a warm bias of about 3°C in the mixed layer and entrainment zone compared to the simulation with the LSM, but this warm bias in the slab model simulation actually helps the PBL temperature in the late morning (e.g., at 1830 UTC). Somewhat ironically, despite the fact that at 1530 UTC the observed PBL is cooler than the two model simulations and both models overestimate the sensible heat flux (see Fig. 1), the observed PBL at local noontime is now warmer than that in the simulations. In other words, the local exchange of surface heat alone cannot explain the rapid warming in the observed PBL in this particular case, and the MM5 failed to capture such a presumably nonlocal effect. Another issue may be associated with the representativeness of FIFE radiosondes, which were launched at a location close to a valley.

To further investigate whether or not the possible drift

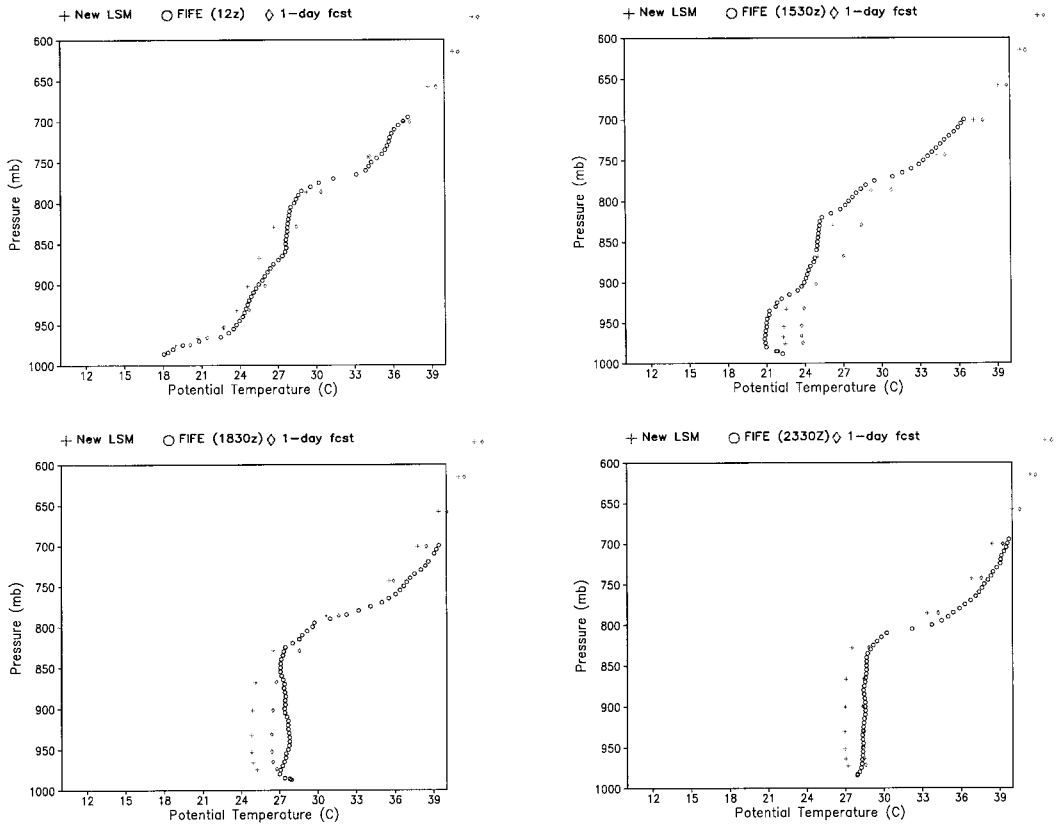

FIG. 8. Comparison of the vertical profile of PBL potential temperature for 5 Jun 1987 between 24–48- and 0–24-h simulations: (a) 1200, (b) 1530, (c) 1830, and (d) 2330 UTC.

in large-scale flow in the MM5 second-day simulation is responsible for this discrepancy, a sensitivity test was conducted with the model being initialized at 0000 UTC 5 June 1987, and the model performed only a 24-h forecast. The results of this simulation are plotted in Fig. 8 and compare with the observation and with the second-day simulation using the same LSM. At 1200 UTC, not long after sunrise, the surface inversion in the 1-day forecast is closer to FIFE observations than that in the second forecast, as expected. However, this 1-day forecast still qualitatively shows the same features seen in the 2-day forecast. That is, the rapid warming of the observed mixed layer in the late morning still has a probable contribution of large-scale advection or changes induced by surface heterogeneity. The 1-day forecast helps, to some extent, the warming of the mixed layer, because the large-scale conditions are expected to be more accurate. Nevertheless, it still fails to capture this rapid warming period.

Figure 9 shows the vertical profile of mixing ratio forecasted by two models and the FIFE observations at the closest corresponding times on 4 June. The structure of the mixing ratio has a similar diurnal cycle to the temperature. Once again, the vertical distribution of humidity in the stable PBL is well captured by both models at 1200 UTC (12 h after the model start). The model lower mixed layer seems to be moistened faster than observations in the early morning, but the modeled upper mixed layer underneath the entrainment zone is drier than the data. As shown in the FIFE data, the mixed layer mixing ratio reaches a maximum at about local noontime, and then falls in the afternoon as the mixed layer deepens further and drier air is entrained from upper layer into the mixed layer. Similar to the evolution of temperature in the PBL, a rapid moistening throughout the entire mixed layer occurs from 1530 to 1830 UTC. Because the modeled latent heat flux in the new LSM simulation closely agrees with the data, such a rapid change of moisture in the data is presumably again due to some nonlocal effects or surface heterogeneity. Interestingly, although the model simulations produce the right mixed layer depth, their mixing ratio is too high compared to the FIFE observations at 2330 UTC. This may imply that the entrainment rate, calculated by the MRF PBL parameterization scheme, is not large enough to get drier air from above, although it seems to be reasonable for temperature evolution. An insufficient entrainment at the boundary layer top is also reported for other PBL parameterizations (e.g., see Betts et al. 1997).

On the next day (Fig. 10), both models have a reasonable moisture distribution in the stable boundary lay-

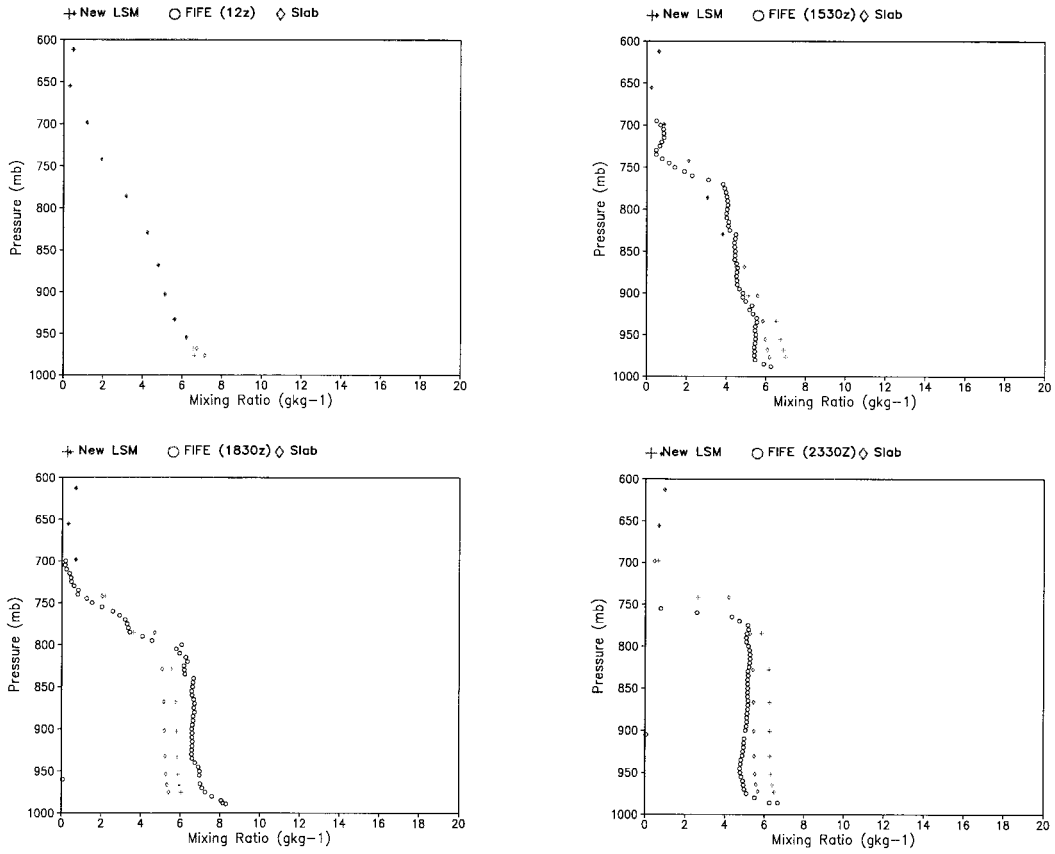

FIG. 9. The vertical profile of mixing ratio in the PBL for 4 Jun 1987: (a) 1200, (b) 1530, (c) 1830, and (d) 2330 UTC.

er, and the new LSM simulation appears to reflect more boundary layer details than the slab model simulation. The reason for the sudden increase of moisture in the lower mixed layer, which occurred from 1200 to 1530 UTC, is still not clear. Although the mixed layer in both models is drier than the data, the moisture profile in the new LSM simulation agrees with the data better than that in the slab model, because of a larger and more reasonable morning evaporation (see Fig. 1c). By the same reasoning, the new LSM model produces a wetter mixed layer than the slab model at 2330 UTC, and the former has also a better agreement with the FIFE data.

Several simulations were conducted to evaluate the sensitivity of PBL development to the initial soil moisture. In these simulations, the initial soil moisture, which is based on the NCEP–NCAR reanalysis, is changed (increased and decreased) by 0.1 in terms of absolute volumetric values, representing a relatively large change in soil moisture. Figures 11 and 12 show comparisons of one simulation (with an increase of 0.1 in initial root zone volumetric soil moisture) with the result of the control simulation for the 4 June case. The evolution of the PBL heights in these simulations is very close to the one in the control simulation. Nonetheless, the vertical profile of temperature and mixing ratio is different. For instance, the simulation with wetter soil produces cooler temperature, but the difference is appreciable only in the afternoon. The maximum difference is less than 2°C at 2330 UTC. As expected, there is a slight increase in the PBL mixing ratio because of more moisture from the surface, but the difference is usually less than 1 g kg^{-1}.

c. Influence of the treatment of land surface processes on precipitation

1) RAINFALL CASE OF 24 JUNE 1997

In this case, at 500 mb, a trough advanced over the upper Midwest states during the 48-h simulated period starting at 0000 UTC 24 June. At the surface a cold front spread southeastward starting in Montana and Wyoming and ending through Missouri, Kansas, and New Mexico. It was associated with temperature drops of 8–10 K, and a continuous band of rainfall mostly as the front crossed Kansas and Iowa in the last 24 h. Ahead of the front Kansas had some convective rainfall in the first 12 h. The strongest rainfall was during the two nights of the period, weakening during the day.

Because of the wide range of scales simulated over

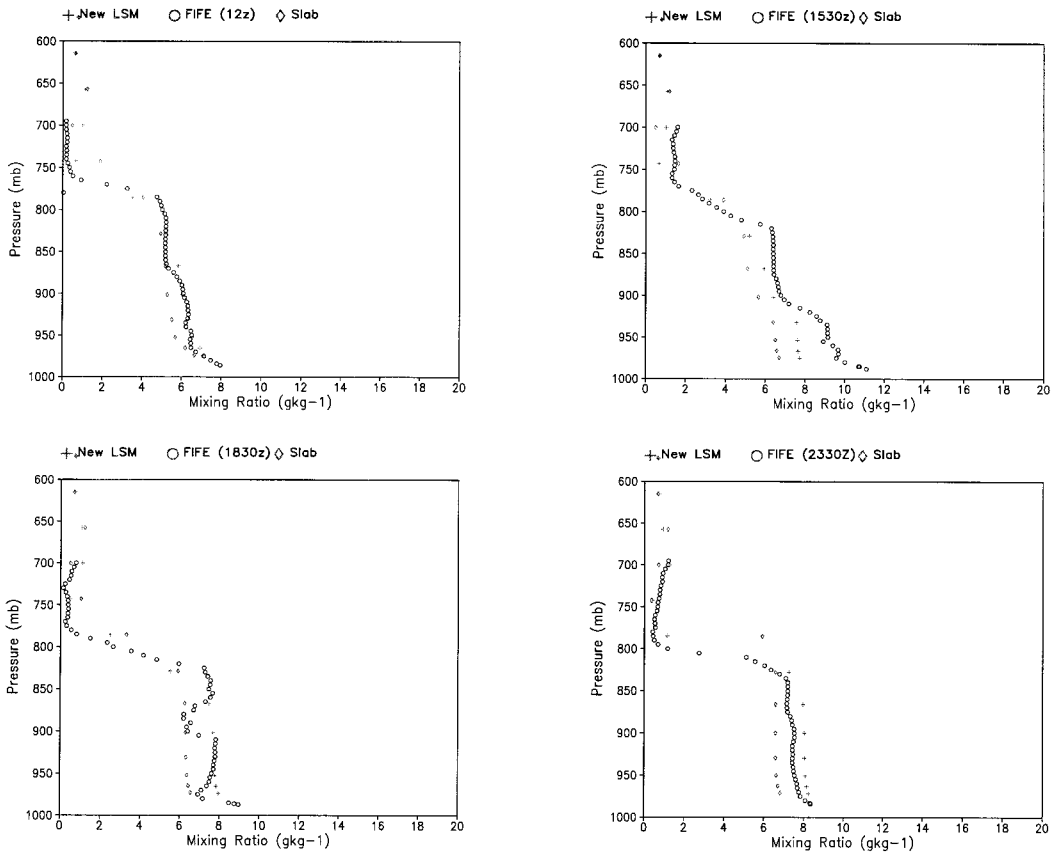

FIG. 10. Same as Fig. 9 but for 5 Jun 1987: (a) 1200, (b) 1530, (c) 1830, and (d) 2330 UTC.

the three model grids, there is an opportunity to evaluate the precipitation forecasts from the synoptic scale to the mesogamma scale. Figure 13 shows the first 12-h (from 0000 to 1200 UTC 24 Jun 1997) rainfall totals simulated by two MM5 simulations with the new LSM and simple slab model, respectively. The same field obtained from NCEP Stage II analysis is also plotted for comparison. It seems that both simulations performed reasonably well in capturing the overall pattern and some of the details in the observed pattern of the 12-h precipitation totals. Specifically, these simulations reflect the heavy rainfall in southern Kansas and over Wyoming. However, the model overpredicts the areal extent of light precipitation, and the simulated rainfall totals are likely too high in the border of northern Wyoming. The placement of heavy rainfall of both model simulations in Nebraska is slightly farther to the southeast compared to observations.

The model rainfall totals from 1200 UTC 24 June to 0000 UTC 25 June (not shown) are very similar in the two model simulations. Compared to observations, the heavy rainfall in Colorado, Nebraska, and Iowa are simulated by both models, but models failed to reproduce the observed convective activity at the border of Colorado and Nebraska. In general, the model tends to overestimate the rainfall. Note that besides the likely model overestimation of rainfall, the NCEP rainfall analysis was underestimated. This is because the latter missed several hours of observations, and there were blackout areas where no gauge and radar observation were available. The rainfall totals from 0000 to 1200 UTC 25 June are slightly different in two model simulations (Fig. 14). Both simulations reasonably reproduce the heavy rainfall band extending from Iowa to Kansas.

Compared to radar analysis, the LSM simulation produced somewhat too much convection in Louisiana, while the rainfall in this area in the slab simulation seems too weak. The Louisiana rain was an isolated cell of convective and nonconvective rain near the boundary of the MM5's domain 2, which existed from 30 to 48 h in the 24 June 1997 case. Only the LSM simulation had this, but both simulations had more rainfall farther east outside domain 2. The LSM may not have any direct effect on this cell. Earlier LSM simulations with older versions of MM5, and different boundary conditions, did not produce this cell, while the slab one did. Thus this particular rainfall event is very sensitive to small effects whether it occurs or not. The boundary layer becomes 1–2 g kg^{-1} moister in the first day for the LSM compared to the slab. This can be traced to high latent heat fluxes around 18 h in southern Louisiana. These high fluxes are not related to particular land use and

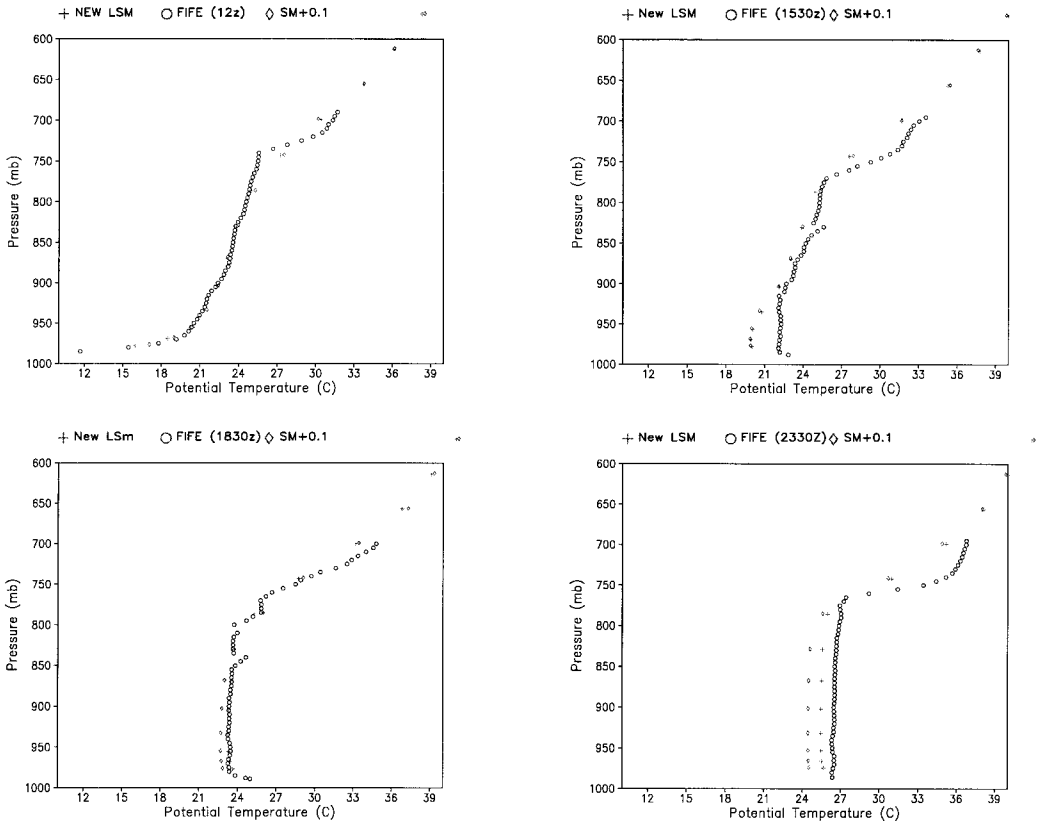

FIG. 11. The vertical profile of potential temperature in the PBL for 4 Jun 1987, obtained from the sensitivity test with an increase of 0.1 in initial root zone soil moisture: (a) 1200, (b) 1530, (c) 1830, and (d) 2330 UTC.

soil texture categories, but are related to a clear slot in the thin low clouds over southern Louisiana at that time. It is difficult to explain why the clear slot appears in the LSM and not with the slab, because the interactions among surface, cloud, and radiation are quite complex. Nevertheless, this maybe responsible for the cell of rainfall later.

2) RAINFALL CASE OF 4 JULY 1997

In this case, a weak 500-mb trough moves eastward out of the Midwest region, and a sharp cold front starts aligned east–west along the Kansas–Oklahoma border at 0000 UTC 4 July. A temperature difference of 10°C occurs across a narrow frontal region. By 1200 UTC the front has descended across Oklahoma, and associated rain also moves south into Texas. The front's motion halts eventually in Texas and in Louisiana and Mississippi. There is some postfrontal rain in Oklahoma on the night of the 4–5 July, and convection starts up by 0000 UTC 6 July at the front in Texas and New Mexico, and farther north in western Kansas.

Rainfall totals for the first 12 h from two simulations are plotted in Fig. 15. Both simulations reasonably reproduce the heavy rainfall in Missouri and Oklahoma, but the isolated convection on the border of Texas and New Mexico appears too weak as compared to the NCEP rainfall analysis. The model rainfall for the next 12 h looks less promising: both models erroneously predict accumulations in northwest Texas, which do not verify. The same model error is also apparent for the next period, where the rainfall in both models has a too large areal extent and an overestimated amount in New Mexico (not shown here).

For heavy precipitation cases forced by large-scale systems, it is generally known that surface fluxes have a small influence on short-range forecasts. This is because the boundary layer properties are determined more by the initial analyses than by surface fluxes. The strength of an improved surface flux would show more in multiday simulations because boundary layer development would depend not only on local surface fluxes, but upstream surface conditions too, and this is the situation in which improved surface flux parameterizations would be most beneficial.

Given that, it is not surprising that both the new land surface model and the slab scheme predict very similar patterns for the heavy frontal rain. The intensity and location are determined by the available boundary layer moisture and the large-scale flow. However, there are subtle improvements in this particular case in regions of the domain that do not have heavy rain. One example

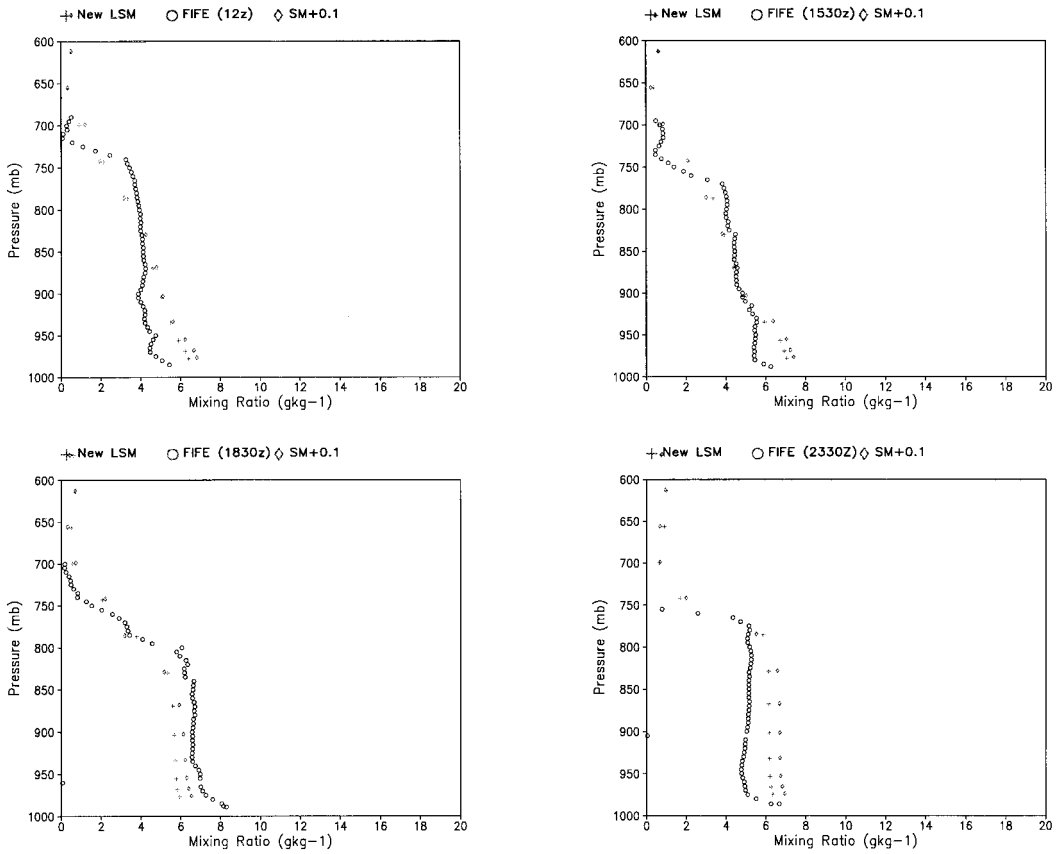

FIG. 12. Same as Fig. 11 but for the mixing ratio in the PBL: (a) 1200, (b) 1530, (c) 1830, and (d) 2330 UTC.

is at 24–27 h of the 4 July 1997 simulation (see Fig. 16). The persistence of rain in Colorado and the suppression of rain on the Oklahoma–Texas border were better handled with the new land surface scheme than with the slab model.

It is very difficult to ascribe a reason for the differences in Colorado. Heterogeneity of the surface near the mountains causes differences in latent heat fluxes, while the treatment of sensible heat flux with skin temperature in the LSM and ground temperature in the slab model appears to cause thermal differences in the boundary layer by 0000 UTC. The LSM run warmed between 2100 and 0000 UTC, while the slab run cooled and moistened in the region where rainfall eventually occurred. Both had a similar temperature at 2100 UTC and a similar moisture at 0000 UTC.

The Oklahoma–Texas rain also was a mixture of convective and resolved-scale rain that occurred after a fairly cloudy day locally in both model runs. This also complicates analysis of the effects of the surface fluxes. Therefore such improvements should be regarded with caution unless a determination is made of the exact mechanism for the improvement in each case.

Both simulations failed to capture a significant mesoscale convective event in western Kansas late on 5 July. This appeared to fail for reasons other than the parameterization of surface properties, because several sensitivity studies in which the LSM run's soil moisture was modified also did not produce the convection. Increasing the soil moisture increases the boundary layer moisture, but also cools it, resulting in little net change in convective available potential energy.

5. Summary

A number of short-term numerical experiments were conducted to evaluate the MM5 model coupled with an advanced land surface model. The performance of the two model systems (one with the default simple slab model and another with a land surface model with explicit vegetation and hydrology treatments) against FIFE observations is documented. For clear sky day cases, the MM5 model gives reasonable estimates of downward solar and downward longwave radiation at the surface, but the solar radiation is slightly overestimated. Such a high bias in downward solar radiation may be due to the lack of aerosol treatment in the current MM5 radiation scheme. The improvements in the calculation of surface latent and sensible heat fluxes with the new LSM are very apparent, and more importantly, the new LSM captures the correct Bowen ratio. Evaporation obtained from the simple slab model is significantly lower

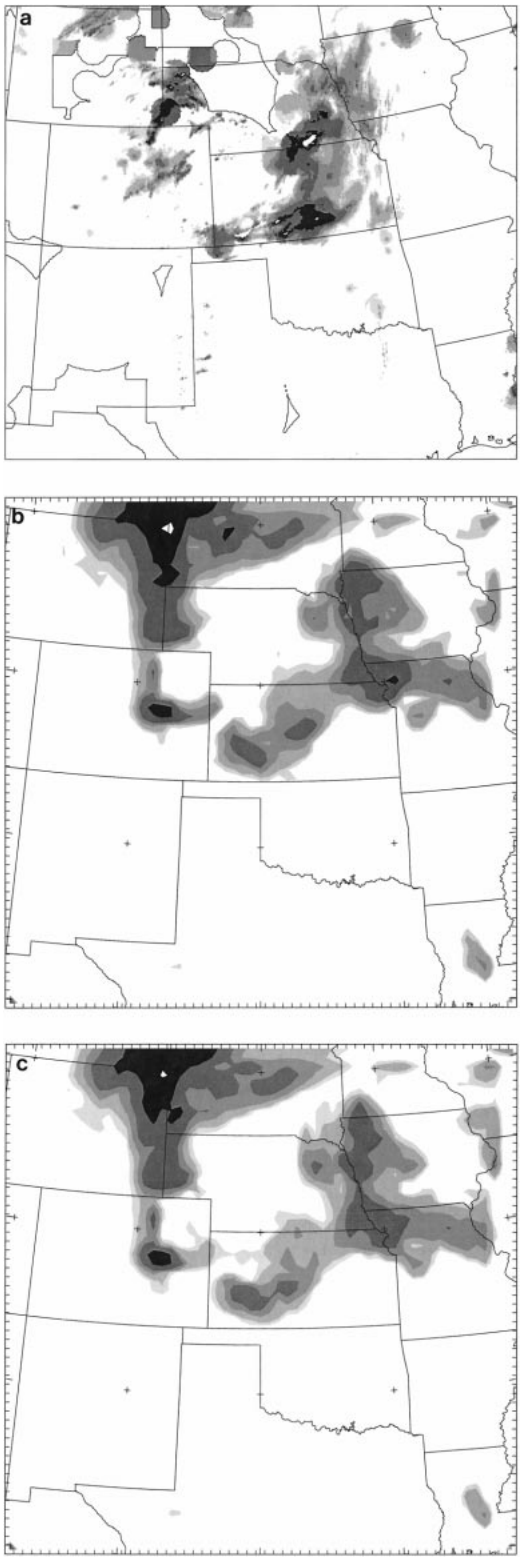

FIG. 13. The 12-h rainfall totals (from 0000 to 1200 UTC 24 Jun 1997): (a) NEXRAD analysis, (b) MM5–LSM model simulation, and (c) MM5–slab model simulation. The contours are <1 mm, white; 1–2 mm, light gray; 2–5 mm, medium gray; 5–10 mm, medium dark gray; 10–25 mm, dark gray; 25–50 mm, black; and >50 mm, white.

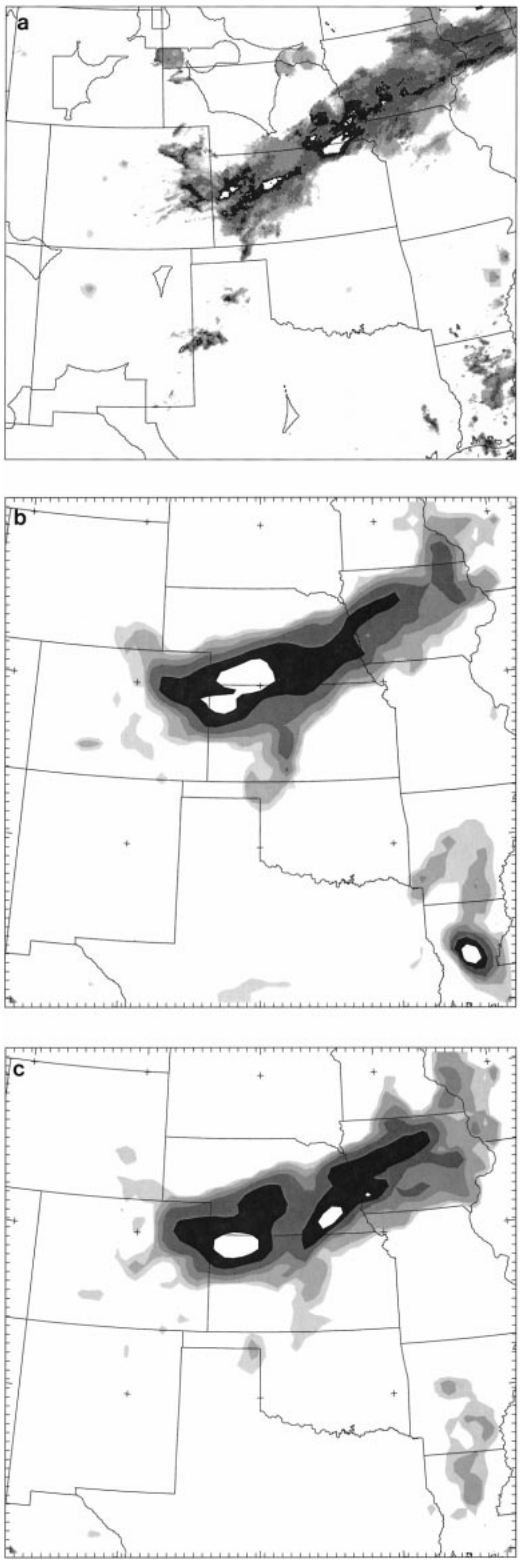

FIG. 14. Same as Fig. 13 but for the 12-h rainfall totals from 0000 to 1200 UTC 25 Jun 1997.

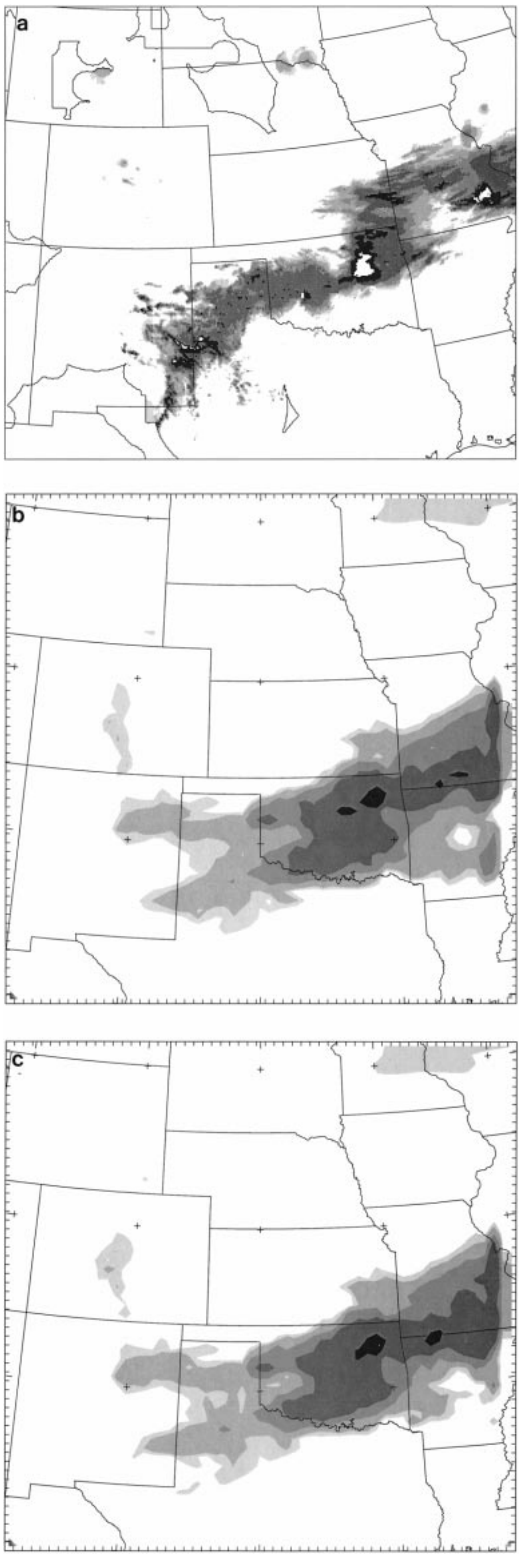

FIG. 15. The 12-h rainfall totals (from 0000 to 1200 UTC 4 Jul 1997): (a) NEXRAD analysis, (b) MM5–LSM model simulation, and (c) MM5–slab model simulation.

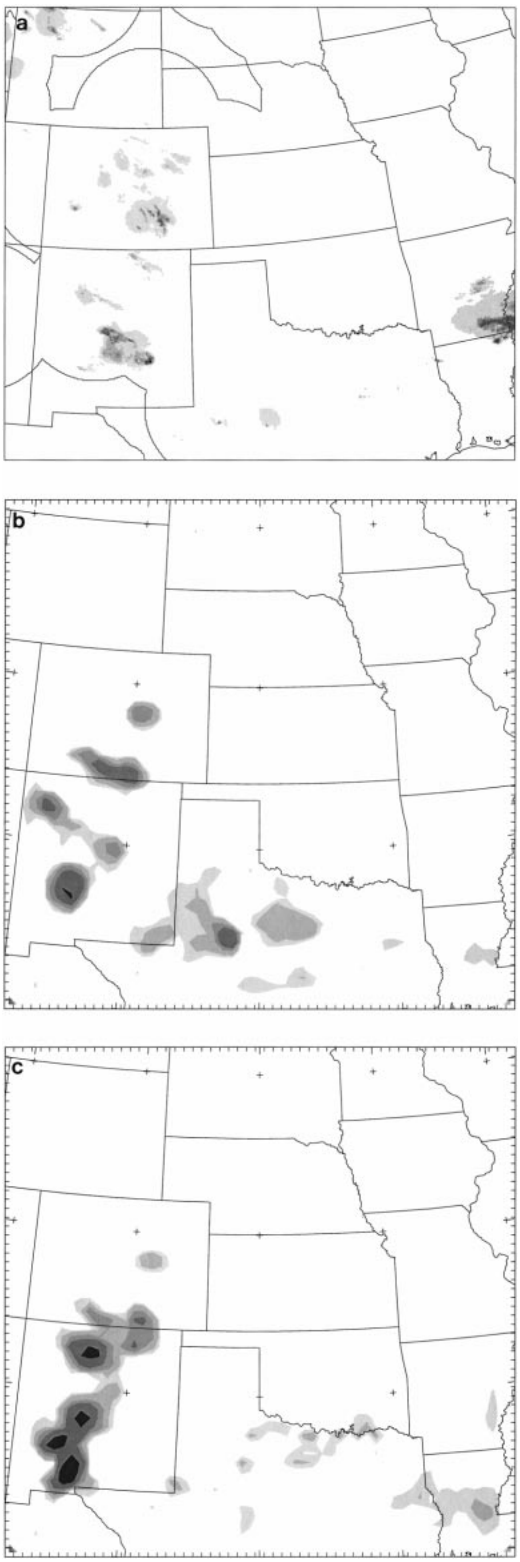

FIG. 16. The 3-h rainfall totals (from 0000 to 0300 UTC 5 Jul 1997): (a) NEXRAD analysis, (b) MM5–LSM model simulation, and (c) MM5–slab model simulation.

than observations. One remarkable feature, which does not verify with observations, is that the latent heat flux in the MM5–slab model increases on the second day of simulation, presumably because of its time-constant soil moisture. Due to the more reasonable diurnal cycle of surface heat fluxes in the MM5–LSM, its near-surface temperature and humidity are closer to the FIFE observations. In particular, the MM5–slab model has a systematic warm bias in 2-m temperature. Also, the MM5–LSM model gives a more reasonable diurnal evolution of near surface humidity.

Demonstrated as well is the difficulty in validating the land surface models on cloudy and rainy days, because modeling the timing and amount of local clouds and precipitation is still a challenging task for mesoscale models. In a case study, model clouds appear too late and too little in the first 18 h of simulation, which resulted in too much surface radiation forcing and hence too much surface heat flux. The opposite appears in the second-day simulation wherein the MM5 model produces too much cloud and has low surface heat fluxes. Another difficulty is associated with the quality of data. For instance, the surface energy balance is not preserved in the field measurements, and it is not easy to distinguish model biases from uncertainties in the data themselves. Some caution must be taken when quantitatively comparing the individual components of surface energy balance.

Both the slab model and the new LSM were coupled with the nonlocal MRF PBL parameterization schemes to assess the daytime evolution of temperature and humidity in the convective PBL. Both models reproduced the depth of morning surface inversion in the stable boundary layer well. On one day, the observed mixed layer in the late morning deepens faster than both models, despite the fact that both models have high bias in surface sensible heat fluxes. Presumably, such a rapid development of convective mixed layer is due to some effects induced by small-scale heterogeneity or large-scale advection that MM5 failed to capture. At local noontime, the MM5–LSM has a slightly better temperature structure in the PBL than the MM5–slab model. Both models reasonably reproduce the daytime convective PBL growth and, in general, the temperature difference between two models and observations is less than 2°C. Both models seem to capture the vertical distribution of mixing ratio in the convective PBL well. Similar to the case of temperature, however, both models fail to reproduce a rapid moistening in the lower mixed layer in the late morning, despite a good estimation of surface latent heat flux in the MM5–LSM model.

The simulations of two rainfall events are not conclusive. Both simulations produce a good forecast of rainfall for 24 June 1997 and have similar problems for the event of 4 July 1997, although the simulations with the new LSM have slightly improved results in some 3-h rainfall accumulations. From these tests we can state that the new LSM does not have unexpected influences in situations for which the land surface processes are secondary, but that it may have subtle, though complex, effects on the model behavior because of heterogeneity introduced by soil moisture, vegetation effects, and soil type, which are all lacking in the slab model. Inclusion of such effects is now possible with the added sophistication of a full land surface model, and the expectation is that the addition of more processes in the model will improve the simulations in a gross sense; that is, taking into account many more cases than we have here.

Finally, this validation study describes the performance of the newly implemented land surface model against several selected cases. It is not, in its nature, an exhaustive study and basically serves to provide some guidelines in terms of implementation strategy and validation for researchers who plan to test different land surface physics in the widely used MM5 modeling system. More studies need to be undertaken to evaluate the importance of the land surface model with higher model resolution and the role of soil moisture and its initialization.

Acknowledgments. This research was supported by the U.S. Army Test and Evaluation Command through an Interagency Agreement with the National Science Foundation, the special funds from the National Science Foundation that have been designated for the U.S. Weather Research Program at NCAR, and DOE/ARM Grant DE-AI02-97ER62359. We express our appreciation to Dr. Thomas Warner for his support and suggestions. We want to thank Lynn Berry for preparing some of the figures used in this article.

REFERENCES

Baldwin, M. E., and K. Mitchell, 1997: The NCEP hourly multisensor U.S. precipitation analysis for operations and GCIP research. Preprints, *13th Conf. on Hydrology*, Long Beach, CA, Amer. Meteor. Soc., 54–55.

Betts, A. K., and J. H. Ball, 1998: FIFE surface climate and site-average dataset 1987–89. *J. Atmos. Sci.,* **55,** 1091–1108.

——, ——, and A. C. M. Beljaars, 1993: Comparison between the land surface response of the ECMWF model and the FIFE-1987 data. *Quart. J. Roy. Meteor. Soc.,* **119,** 975–1001.

——, F. Chen, K. Mitchell, and Z. Janjic, 1997: Assessment of land surface and boundary layer models in two operational versions of the Eta Model using FIFE data. *Mon. Wea. Rev.,* **125,** 2896–2915.

Blackadar, A. K., 1976: Modeling the nocturnal boundary layer. Preprints, *Third Symp. on Atmospheric Turbulence, Diffusion and Air Quality,* Raleigh, NC, Amer. Meteor. Soc, 46–49.

——, 1979: High resolution models of the planetary boundary layer. *Advances in Environmental Science and Engineering,* J. Pfafflin and E. Ziegler, Eds., Vol. 1, No. 1, Gordon and Breach, 50–85.

Chen, F., and J. Dudhia, 2001: Coupling an advanced land surface–hydrology model with the Penn State–NCAR MM5 modeling system. Part I: Model implementation and sensitivity. *Mon. Wea. Rev.,* **129,** 569–585.

——, and Coauthors, 1996: Modeling of land-surface evaporation by four schemes and comparison with FIFE observations. *J. Geophys. Res.,* **101,** 7251–7268.

——, ——, Z. Janjic, and M. Baldwin, 1997: Coupling a land-surface

model to the NCEP mesoscale Eta model. Preprints, *l3th Conf. on Hydrology,* Long Beach, CA, Amer. Meteor. Soc., 99–100.

Chen, T. H., and Coauthors, 1997: Cabauw experimental results from the Project for Intercomparison of Land-surface Parameterization Schemes. *J. Climate,* **10,** 1194–1215.

Davis, C., T. Warner, E. Astling, and J. Bowers, 1999: Development and application of an operational relocatable, mesogamma-scale weather analysis and forecasting system. *Tellus,* **51A,** 710–727.

Dudhia, J., 1989: Numerical study of convection observed during the Winter Monsoon Experiment using a mesoscale two-dimensional model. *J. Atmos. Sci.,* **46,** 3077–3107.

Grell, G., J. Dudhia, and D. Stauffer, 1994: A description of the Fifth-Generation Penn State/NCAR Mesoscale Model (MM5). NCAR Tech. Note. NCAR/TN-398+STR, 117 pp.

Hong, S.-Y., and H.-L. Pan, 1996: Nonlocal boundary layer vertical diffusion in a medium-range forecast model. *Mon. Wea. Rev.,* **124,** 2322–2339.

Jacquemin, B., and J. Noilhan, 1990: Sensitivity study and validation of a land surface parameterization using the HAPEX-MOBILHY data set. *Bound.-Layer Meteor.,* **52,** 93–134.

Kalnay, E., and Coauthors, 1996: The NCEP/NCAR 40-Year Reanalysis Project. *Bull. Amer. Meteor. Soc.,* **77,** 437–471.

Mahrt, L., and M. Ek, 1984: The influence of atmospheric stability on potential evaporation. *J. Climate Appl. Meteor.,* **23,** 222–234.

——, and H. L. Pan, 1984: A two-layer model of soil hydrology. *Bound.-Layer Meteor.,* **29,** 1–20.

Pan, H.-L., and L. Mahrt, 1987: Interaction between soil hydrology and boundary-layer development. *Bound.-Layer Meteor.,* **38,** 185–202.

Schaake, J. C., V. I. Koren, Q. Y. Duan, K. Mitchell, and F. Chen, 1996: A simple water balance (SWB) model for different spatial and temporal scales. *J. Geophys. Res.,* **101,** 7461–7475.

Sellers, P. J., F. G. Hall, G. Asrar, D. E. Strebel, and F. F. Murphy, 1992: An overview of the First International Satellite Land Surface Climatology Project (ISLSCP) Field Experiment (FIFE). *J. Geophys. Res.,* **97,** 18 345–18 371.

Strebel, D. E., D. R. Landis, K. F. Huemmerich, and B. W. Meeson, 1994: Collected data of the First ISLSCP Field Experiment. *Surface Observations and Nonimage Data Sets,* Vol. 1, NASA Goddard Space Flight Center, CD-ROM.

Sugita, M., and W. Brutsaert, 1990: How similar are temperature and humidity profiles in the unstable boundary layer? *J. Appl. Meteor.,* **29,** 489–497.

Troen, I., and L. Mahrt, 1986: A simple model of the atmospheric boundary layer: Sensitivity to surface evaporation. *Bound.-Layer Meteor.,* **37,** 129–148.

Viterbo, P., and A. C. Beljaars, 1995: An improved land surface parameterization scheme in the ECMWF model and its validation. *J. Climate,* **8,** 2716–2748.

Zhang, D.-L., and R. A. Anthes, 1982: A high-resolution model of the planetary boundary layer—Sensitivity tests and comparisons with SESAME-79 data. *J. Appl. Meteor.,* **21,** 1594–1609.